2008

A Simplified Steady-State Model for Predicting the Energy Consumption of Household Refrigerators and Freezers

Joaquim M. Gonzalves
Federal University of Santa Catarina

Christian J. L. Hermes
Federal University of Santa Catarina

Claudio Melo
Federal University of Santa Catarina

Fernando T. Knabben
Federal University of Santa Catarina

Follow this and additional works at: http://docs.lib.purdue.edu/iracc

A Simplified Steady-State Model for Predicting the Energy Consumption of Household Refrigerators and Freezers

Joaquim M. GONÇALVES[*], Christian J. L. HERMES, Cláudio MELO, Fernando T. KNABBEN

POLO Research Laboratories for Emerging Technologies in Cooling and Thermophysics,
Federal University of Santa Catarina, 88040-900, Florianópolis, SC, Brazil
Phone: +55 48 3234 5691, e-mail: hermes@polo.ufsc.br

[*] HVAC&R Research Group, Federal Center of Technological Education of Santa Catarina,
Rua José Lino Kretzer 608, 88103-310, São José, SC, Brazil

ABSTRACT

A simplified model to assess the energy performance of vapor compression refrigerators and freezers is presented herein. The model consists of first-principles algebraic equations adjusted with experimental information obtained from the refrigeration system under study. The experimental work consisted of controlling and measuring the system and component operating conditions in order to gather key information for the development and validation of the model. The methodology showed similar accuracy to that using more sophisticated dynamic simulation codes, but with lower computational costs. When compared to experimental data, the model predicted AHAM energy consumption tests within a ±5% deviation band. A sensitivity analysis considering the number of tube rows in the condenser coil, the number of fins in the evaporator coil and the compressor stroke is also reported. The refrigeration system under study was a top-mount 'Combi' 600-liter refrigerator, on-off controlled by the fresh-food compartment temperature.

1. INTRODUCTION

Component matching and energy assessment of household refrigeration systems are usually carried out through costly, time consuming standardized test procedures (e.g., AHAM HRF-1, 2004; ISO15502, 2005). In order to speed up the product development process, first-principles simulation models have been employed to simulate the thermo-hydrodynamic behavior of these appliances. Steady-state and transient approaches have both been used, the former for component matching (e.g., Davis and Scott, 1976; Abramson *et al.*, 1990; Klein *et al.*, 1999; Gonçalves and Melo, 2004), and the latter essentially to assess energy performance (e.g., Melo *et al.* 1988, Jansen *et al.* 1988, Jakobsen, 1995; Hermes and Melo, 2006).

In a previous study, Gonçalves and Melo (2004) investigated the steady-state behavior of a top-mount refrigerator by measuring and modeling the performance characteristics of each of its components. The models were based on the mass, energy and momentum conservation principles and also on empirical data. Measurements of the relevant variables were taken at several positions along the refrigeration loop, generating performance data not only for the whole unit but also for each of the cycle components. The experiments were planned and performed following a statistical methodology and considering 13 independent variables that led to over 160 data runs. The model predictions for the cooling capacity and power consumption, when compared with experimental data, were within a ±10% deviation band. The model was also used to simulate the effect of the system parameters on the refrigerator performance in an attempt to minimize the power consumption for a given internal air temperature. However, the steady-state model of Gonçalves and Melo (2004) is not suitable for predicting the refrigerator energy consumption, since this is dependent not only on the power consumption, but also on the compressor runtime.

Later, Hermes and Melo (2006) put forward a first-principles model for simulating the transient behavior of household refrigerators. The model was used to simulate a typical top-mount refrigerator, where the compressor is on-off controlled by the freezer temperature, while a thermo-mechanical damper is used to set the fresh-food

compartment temperature. Innovative modeling approaches were proposed for each of the refrigerator components (condenser, evaporator, compressor, capillary tube-suction line heat exchanger, and refrigerated compartments). Numerical predictions were compared to experimental data showing a reasonable level of agreement for the whole range of operating conditions, including the start-up and cycling regimes. The system energy consumption was found to be within ±10% agreement with the experimental data, while the compartment air temperatures were predicted with a maximum deviation of ±1°C. The model was also used to assess the impact of some operational and geometric parameters on the overall energy consumption. The code, however, requires a considerable amount of CPU time, not being viable for optimization tasks that may require thousands of runs in a row.

In order to address this drawback, a simplified methodology for predicting the energy consumption of household refrigerators and freezers with a similar accuracy, but with a substantially lower computational effort than that required by the dynamic simulation code of Hermes and Melo (2006), is proposed herein. The model followed the steady-state semi-empirical approach introduced by Gonçalves and Melo (2004), but was adapted to estimate the refrigerator runtime as a function of the cabinet thermal loads and cooling capacity.

2. MATHEMATICAL MODEL

The mathematical formulation follows closely that introduced by Gonçalves and Melo (2004), according to which the refrigeration system was divided into the following sub-domains: compressor, heat exchangers (evaporator and condenser), capillary tube-suction line heat exchanger, evaporator and condenser fans, and refrigerated compartments, as depicted in Fig. 1.
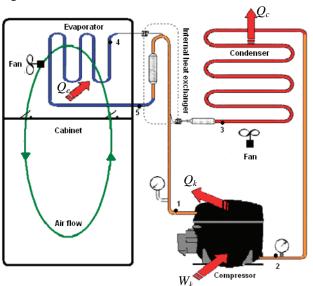

Figure 1. Schematic representation of a top-mount refrigerator

2.1 Compressor
The refrigerant enthalpy at the compressor discharge, h_2, was calculated from an energy balance in the compressor shell, as follows

$$h_2 = h_1 + (W_k - Q_k)/m \qquad (1)$$

The compressor mass flow rate, m, was obtained from equation (2), where η_v stands for the volumetric efficiency,

$$m = \eta_v V_k N / v_1 \qquad (2)$$

The compression power, W_k, was obtained from equation (3), where η_g corresponds to the compressor overall efficiency,

$$W_k = m(h_{2,s} - h_1)/\eta_g \qquad (3)$$

The heat released by the compressor shell to the surroundings, Q_k, was calculated from

$$Q_k = UA_k (T_2 - T_a) \tag{4}$$

The volumetric and overall efficiencies, η_v and η_g, and the overall thermal conductance, UA_k, were all obtained from experimental tests carried out with the refrigerator. The volumetric and overall efficiencies were fitted as linear functions of the pressure ratio, p_c/p_e, while the thermal conductance UA_k was assumed to be constant.

2.2 Capillary tube-suction line heat exchanger

The refrigerant enthalpy at the capillary tube exit, h_4, was obtained from an energy balance in the capillary tube-suction line heat exchanger (see Fig. 1),

$$h_4 = h_3 + h_5 - h_1 \tag{5}$$

The suction line exit temperature, T_1, was calculated from equation (6), where the heat exchanger effectiveness, ε, was derived from experimental tests carried out with the refrigerator,

$$T_1 = T_5 + \varepsilon (T_3 - T_5) \tag{6}$$

2.3 Heat exchangers

2.3.1 Thermal model

The heat exchangers (condenser and evaporator) were divided into sub-regions according to the thermodynamic state of the refrigerant. The condenser was divided into three different regions (superheating, saturation and subcooling), whilst the evaporator was divided into two regions (saturation and superheating). The heat exchanger coils were assumed to be straight and horizontal, with uniformly distributed fins. The coils were divided into N control volumes. The heat transferred was calculated by applying equations (7) to (9) to each of the control volumes,

$$Q_x = m(h_{i,x} - h_{o,x}) = \varepsilon C_{min} \Delta T_{max} \tag{7}$$

where ε is the temperature effectiveness of the cross-flow heat exchanger, expressed as a function of the number of transfer units, $NTU = UA_x/C_{min}$, and of the ratio between the refrigerant and air-side thermal capacities, $C_{ratio} = C_{min}/C_{max}$ (Kays and London, 1998). The effectiveness of the two and single-phase flow regions were calculated as follows,

$$\varepsilon = 1 - exp(-NTU) \tag{8}$$
$$\varepsilon = 1 - exp\{-[1 - exp(-C_{ratio} NTU)]/C_{ratio}\} \tag{9}$$

The overall thermal conductance, UA_x, was calculated from

$$UA_x^{-1} = (\alpha_i A_i)^{-1} + (\eta_e \alpha_e A_e)^{-1} \tag{10}$$

The tube wall and the tube-fin contact thermal resistances were both neglected. An infinite internal heat transfer coefficient, α_i, was adopted for the two-phase flow regions, whilst Gnielinski's correlation (1976) was employed for the single-phase regions. The length of each flow region was determined by comparing the local refrigerant enthalpy with that of saturated vapor or saturated liquid. The wire-and-tube condenser and the tube-fin 'no-frost' evaporator external heat transfer coefficients, α_e, were calculated using the correlations of Petroski and Clausing (1999) and Kim *et al.* (1999), respectively. The fin efficiencies were determined by Schmidt's method (1945).

2.3.2 Air flow model

The air-side pressure drop of the heat exchangers were calculated from

$$\Delta p_x = K_x \rho_a \dot{V}_x^2 \tag{11}$$

The bypass air was also taken into account by considering that

$$\Delta p_x = \Delta p_{bypass} = K_{bypass} \rho_a V_x^2 \tag{12}$$

The overall air flow rate V_x was calculated iteratively from equations (11) and (12). The condenser pressure loss coefficient K_x was obtained from tests carried out in a wind-tunnel facility, whereas the evaporator pressure drop was estimated by Kim *et al.*'s correlation (1999). The condenser and evaporator fans were modeled by 6th-order polynomial fits of Δp_{xf} and η_{xf} as functions of the air flow rate, V_x. The pumping power was calculated as follows,

$$W_{xf} = \Delta p_{xf} V_x / \eta_{xf} \tag{13}$$

2.4 Refrigerated compartments

2.4.1 Thermal model
Figures 2 and 3 respectively show schematic representations of the energy and fluid flows within the refrigerated compartments. The evaporator air mass flow rate, m_{ef}, is split into two air streams by a damper action; part of the air is supplied to the freezer compartment, m_{fz}, and part to the fresh-food compartment, m_{ff}. An energy balance involving the evaporator, the freezer and fresh-food compartments yields (see Fig. 2),

$$r\left(Q_e - W_{ef}\right) = UA_{fz}\left(T_a - T_{fz}\right) + R_m^{-1}\left(T_{ff} - T_{fz}\right) \tag{14}$$
$$\left(1 - r\right)\left(Q_e - W_{ef}\right) = UA_{ff}\left(T_a - T_{ff}\right) - R_m^{-1}\left(T_{ff} - T_{fz}\right) \tag{15}$$

where $r = m_{fz}/m_{ef}$ is the freezer air flow rate fraction, UA_{fz} and UA_{ff} are the overall thermal conductances of the freezer and fresh-food compartments, and R_m is the mullion thermal resistance, defined as

$$R_m^{-1} = r\left(1 - r\right)m_{ef} c_{pa} + UA_m \tag{16}$$
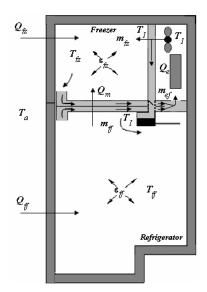

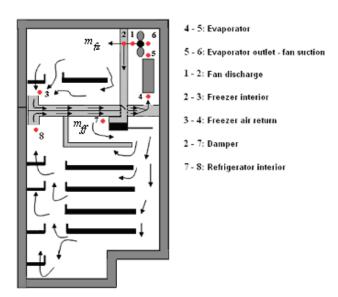Figure 2. Heat flow within the refrigerated compartments

Figure 3. Fluid flow within the refrigerated compartments

It is worth noting that the compartment temperatures are design conditions (ISO: T_{ff}=5°C and T_{fz}=-18°C; AHAM T_{ff}=7.2°C and T_{fz}=-15°C) that need to be specified by the user. Equations (14) to (16) must then be solved for the freezer air fraction, r, a parameter that balances the air flow between the freezer and fresh-food compartments. Finally, the air temperature at the evaporator inlet is calculated from

$$T_m = rT_{fz} + \left(1 - r\right)T_{ff} \tag{17}$$

2.4.2 Air flow model
The air-side pressure drop in each branch of the refrigerated compartments (see Fig. 3) was computed using equation (11), where the pressure loss factor, K_x, was obtained from wind-tunnel experiments. The pressure loss from the evaporator inlet to the fan outlet is given by

$$\Delta p_{4-1} = \Delta p_{ef} - \Delta p_{4-5} - \Delta p_{5-6} \tag{18}$$

where Δp_{ef} is the fan pressure rise, and Δp_{4-1} corresponds to the pressure drops in both the freezer and fresh-food compartments,

$$\Delta p_{4-1} = \Delta p_{1-2} + \Delta p_{2-3} + \Delta p_{3-4} \tag{19}$$

The hydrodynamic coupling between the evaporator, the evaporator fan, and the refrigerated compartments is given by equations (18) and (19) which, when solved, provide the evaporator air flow rate.

2.5 Energy consumption calculation

The energy consumption of a thermostat-controlled refrigerator is calculated by integrating the overall power consumption during a running cycle. Assuming that both the thermal load, Q_t, and the cooling capacity, Q_e, are nearly constant during the cycling regime, the energy consumption can be estimated by an approximated runtime ratio, calculated from the following energy balance over a running cycle,

$$\tau \equiv t_{on} / \left(t_{on} + t_{off} \right) \cong Q_t / Q_e \tag{20}$$

Thus, the overall energy consumption can be easily calculated from

$$Energy = \tau \left(W_k + W_{ef} + W_{cf} \right) \tag{21}$$

where W_k, W_{ef} and W_{cf} are the power required by the compressor, evaporator fan and condenser fan, respectively.

2.6 Determination of the working pressures

Two additional equations are required to determine the evaporating and condensing pressures. In general, the working pressures are obtained implicitly and iteratively from the following mass balances,

$$m - m' = 0 \tag{22}$$

$$M - \sum_n M_n = 0 \tag{23}$$

where m and m' are the compressor and the expansion device (not modeled) mass flow rates, respectively, M is the actual refrigerant charge and M_n is the calculated amount of refrigerant in each of the n components of the refrigeration loop (not modeled). It is worth noting that equations (22) and (23) are strongly non-linear functions of the working pressures, leading to time-consuming solutions and also to convergence issues. In order to keep a reasonable level of complexity, equations (22) and (23) were replaced by fixed values of refrigerant superheating and subcooling at the evaporator and condenser exits, respectively. The working pressures were then calculated straightforwardly from,

$$p_e = p_{sat} \left(T_5 - \Delta T_{sup} \right) \tag{24}$$

$$p_c = p_{sat} \left(T_3 + \Delta T_{sub} \right) \tag{25}$$

This procedure not only eliminates potential convergence issues, but also brings the numerical analysis closer to the design practice, where both the capillary tube and the refrigerant charge are adjusted *a posteriori* to guarantee a certain degree of superheating and subcooling.

3. SOLUTION ALGORITHM

The solution algorithm consists of two iterative loops. In the outer loop, the condensing and evaporating pressures, the refrigerant temperature at the compressor inlet and the air temperature at the evaporator inlet are calculated by the Newton-Raphson method. In the inner loop, a successive substitution strategy was adopted for each of the system components. Thus, for a given set of values for p_e, p_c, h_1 and T_m, the compressor sub-model calculates h_2, the condenser sub-model estimates h_3 and $T_3=T(p_c,h_3)$, the internal heat exchanger sub-model calculates h_4 and T_1, and the evaporator sub-model calculates h_5 and $T_5=T(p_e,h_5)$. Finally, the cabinet thermal and hydraulic models are solved to estimate both r and τ. The calculation procedure continues until convergence is achieved. The code was implemented using the EES platform (Klein, 2002) connected to REFPROP7 software (Lemmon *et al.*, 2002).

4. EXPERIMENTAL WORK

The refrigerator was instrumented and installed inside an environmental chamber with controlled air temperature and humidity. Type T thermocouple probes immersed in the refrigerant flow passage and absolute pressure transducers were installed at three points along the refrigeration loop: compressor suction and discharge ports, and the condenser exit section. A Coriolis-type mass flow meter was installed in the discharge line. The outside air temperature was measured by 5 thermocouples placed around the refrigerator. The freezer and the fresh food compartment air temperatures were measured by 3 and 5 thermocouples placed inside the compartments, respectively. Air-side temperatures at the heat exchanger inlet and outlet ports were also measured. The compressor, evaporator fan and condenser fan power consumptions were also monitored. Tests were carried out before and after the instrumentation set-up to check for any effect on system performance. The system employed HFC-134a as the working fluid (110 g).

Firstly, steady-state tests were carried out for three different ambient temperatures 25°C, 32°C and 43°C to acquire data required to adjust the model empirical parameters (e.g., cabinet thermal conductance). Later, 10 energy consumption tests (ANSI/AHAM, 2004) were carried out with different thermostat and damper settings to validate the model. In addition, the air-side pressure drops at several parts of the refrigerated compartments and also along the heat exchangers (condenser and evaporator) were evaluated using a wind-tunnel test facility (Barbosa *et al.*, 2008). The wind-tunnel was also employed to evaluate the characteristic curves of both fans.

5. RESULTS

The model was validated by supplying the measured average cabinet air temperatures and the superheating and subcooling degrees as input data. Table 1 compares the energy consumption model predictions with their experimental counterparts. It can be noted that a consistent agreement was achieved, with all values falling inside a ±5% error band. Some simulations were also performed to assess the impact of some design parameters on the refrigerator performance. All simulations were carried out based on the AHAM test conditions, and using a fixed subcooling and superheating of 3°C and an internal heat exchanger effectiveness of 0.85.

Table 1. Predicted versus measured energy consumption values

Test #	Measured [kWh/month]	Predicted [kWh/month]	Error [%]
1	35.2	37.0	5.1
2	52.8	50.2	-5.0
3	37.0	37.3	1.0
4	48.5	48.1	-0.8
5	37.6	36.0	-4.3
6	38.4	36.9	-4.0
7	36.7	36.2	-1.4
8	37.4	36.5	-2.4
9	37.5	36.9	-1.6
10	38.3	37.2	-3.0

Figure 4 shows the energy consumption as a function of compressor stroke, but keeping the compressor efficiency constant. It is worth noting that the resultant behavior is quasi linear and that the energy consumption dropped by 13% when the piston displacement was reduced from 5.96 to 3.77 cm^3. This is so because the original compressor cooling capacity is a bit excessive. The same kind of analysis was carried out, but using different compressors with different capacities and efficiencies (see Fig. 5). The nominal capacities shown in Fig. 5 refer to the following compressor calorimeter testing conditions: T_c=55°C, T_e=-25°C, T_1=32°C, and T_a=32°C. Figure 5 shows that the energy consumption dropped by 4.5%, when the original compressor (#2) was replaced by a lower capacity, same efficiency compressor (#3). On the other hand, a lower capacity, lower efficiency compressor (#5) provided an energy performance similar to that obtained with compressor #3. Moreover, a higher capacity, lower efficiency compressor (#1) increased the energy consumption by 20%. Figure 6 explores the effect of the number of tube rows in the condenser coil on the system performance. It can be seen that the energy consumption was reduced by 4% when the number of condenser tube rows was increased from 18 to 24. It is clear that the augmentation of the heat transfer surface overcame the increase in the air-side pressure drop, improving the condenser performance. Figure 7

shows that the energy consumption practically does not change when more fins are added to the evaporator, but increases by 2% when 10 fins are removed from the evaporator coil.
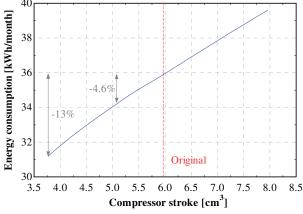

Figure 4. Effect of compressor stroke on the energy consumption: constant efficiency
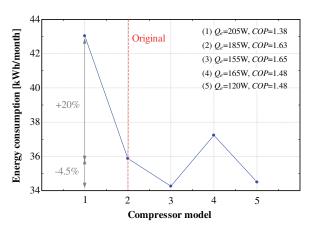

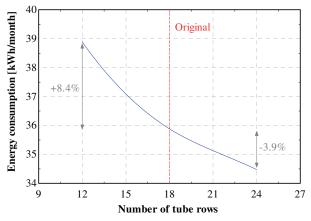Figure 5. Effect of compressor stroke on the energy consumption: real compressors

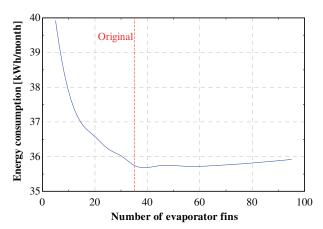Figure 6. Effect of condenser tube rows on the energy consumption

Figure 7. Effect of evaporator fin on the energy consumption

6. CONCLUSIONS

A simplified methodology for predicting the energy consumption of refrigerators and freezers using a first-principles steady-state simulation model was proposed and validated against experimental AHAM energy consumption data. The model predictions were compared with their experimental counterparts, showing agreement within a ±5% error band. Additionally, the model was used to assess the energy performance of a 'Combi' refrigerator in terms of the compressor stroke, the number of condenser tube rows, and the number of evaporator fins. It was shown that the product energy consumption can be decreased by as much as 7.5% by using a lower capacity compressor and at the same time adding 6 more tube rows in the condenser coil. Clearly, the economic feasibility of these modifications needs to be addressed. It should be emphasized that the model requires less than 1 min of CPU time (Intel Core 2 Duo 1.86GHz 2Gb RAM PC) to carry out an energy consumption prediction, a value substantially lower than that required by more sophisticated dynamic simulation models.

NOMENCLATURE

Roman

A	area (m^2)		h	specific enthalpy (J/kg)
C	thermal capacity (W/K)		m	mass flow rate (kg/s)
			M	refrigerant charge (g)

N	compressor speed (s^{-1})		η	efficiency (-)
NTU	number of transfer units (-)		ρ	density (kg/m^3)
p	pressure (Pa)		τ	runtime ratio (-)
Q	heat transfer rate (W)			
r	fraction of air flow to the freezer compartment (-)		**Subscripts**	
T	temperature (K)		a	air, ambient
t	time (s)		c	condensing
UA	overall thermal conductance (W/K)		e	evaporating, external
v	specific volume (m^3/kg)		ff	fresh-food compartment
V	air flow rate (m^3/s)		fz	freezer compartment
V_k	compressor displacement (m^3)		i	internal, inlet
W	power (W)		k	compressor
			m	mixture, mullion
Greek			o	outlet
α	heat transfer coefficient (W/m^{2}K)		x	heat exchangers
ε	heat exchanger effectiveness (-)		xf	heat exchanger fan

REFERENCES

Abramson DS, Turiel I, Heydari A, 1990, Analysis of Refrigerator-Freezer Design and Energy Efficiency by Computer Modeling: DOE Perspective, ASHRAE Transactions, Vol. 96, Part I, pp.1354-1358

ANSI/AHAM HRF-1, 2004, Energy performance and capacity of household refrigerators, refrigerator-freezers and freezers, American National Standards Institute, Washington-DC, USA

Barbosa Jr. JR, Melo C, Hermes CJL, 2008, A study of air-side heat transfer and pressure drop characteristics of tube-fin 'no-frost' evaporators, International Refrigeration and Air Conditioning Conference at Purdue, West Lafayette-IN, USA, Paper 2310

Davis GL, Scott TC, 1976, Component Modeling Requirements for Refrigeration System Simulation: Large Effort, Little Effect?, Compressor Technology Conference at Purdue, West Lafayette-IN, USA, pp.401-408

Gnielinski V, 1976, New equations for heat and mass transfer in turbulent pipe and channel flow, International Chemical Engineering, Vol. 16, No. 2, pp. 359-368

Gonçalves JM, Melo C, 2004, Experimental and numerical steady-state analysis of a top-mount refrigerator, Int. Refrigeration Conference at Purdue, West Lafayette-IN, USA, Paper R078

Hermes CJL, Melo C, 2006, A dynamic simulation model for fan-and-damper controlled refrigerators, 11th International Refrigeration Conference at Purdue, West Lafayette, USA, Paper R036

ISO/FDIS 15502, 2005, Household refrigerating appliances - Characteristics and test methods, International Organization for Standardization, Geneva, Switzerland

Jakobsen A, 1995, Energy optimisation of refrigeration systems: the domestic refrigerator – a case study, *PhD thesis*, Technical University of Denmark, Lyngby, Denmark

Jansen MJP, Kuijpers LJM, de Wit JA, 1988, Theoretical and experimental investigation of a dynamic model for small refrigerating systems, *IIR/IIF Meeting at Purdue*, pp. 245-255

Kays WM, London AL, 1998, Compact heat exchanger, Krieger Publishing, Boca Raton-FL, USA

Kim NH, Youn B, Webb RL, 1999, Air-side heat transfer and friction correlations for plain fin-and-tube heat exchangers with staggered tube arrangements, Transactions of the ASME, J. Heat Transfer, 121, pp.662-667

Klein FH, Melo C, Marco ME, 1999, Steady-State Simulation of an All Refrigerator, 20th International Congress of Refrigeration, Sydney, 1999, Vol. III, Paper 073

Klein SA, 2002, EES – Engineering Equation Solver User's Manual, F-Chart Software, Middleton, WI, USA

Lemmon EW, McLinden MO, Huber M.L., 2002, NIST Reference fluids thermodynamic and transport properties – REFPROP 7.0, National Institute of Standards and Technology, Gaithersburg, MD, USA

Melo C, Ferreira RTS, Negrão COR, Pereira RH, 1988, Dynamic behaviour of a vapour compression refrigerator: a theoretical and experimental analysis, *IIR/IIF Meeting at Purdue*, West Lafayette, USA, pp.98-106

Petroski SJ, Clausing AM, 1999, An investigation of the performance of confined, saw-tooth shaped wire-on-tube condensers, Technical Report ACRC TR-153, University of Illinois, Urbana-IL, USA

Schmidt TE, 1945, La production calorifique dês surfaces munies d'ailettes, Bulletin de IIF, Annexe G-5

ACKNOWLEDGEMENTS